
Structure and Dynamics of a Lattice of Tetragonal Germanates $R_2Ge_2O_7$ (R = Tb–Lu, Y): Ab Initio Calculation

V. S. Ryumshin^{a, *} and V. A. Chernyshev^a

^a Ural Federal University, Yekaterinburg, 620002 Russia

*e-mail: krios_two@mail.ru

Abstract—The crystal structure, phonon spectrum, and elastic constants of a series of rare-earth germanates (including yttrium germanate $R_2Ge_2O_7$ (R = Tb–Lu, Y)) with a tetragonal structure have been ab initio calculated within the density functional theory. The frequencies and types of fundamental vibrations and the intensities of IR and Raman modes are determined. The degrees of participation of ions in each mode are determined by analyzing the displacement vectors obtained as a result of the ab initio calculations. The calculations have been performed for the first time; there are no corresponding experimental data for the entire series of compounds (except for the IR and Raman spectra of yttrium germanate). The performed calculations made it possible to interpret and supplement the known data in the literature on IR and Raman spectra of yttrium germanate $Y_2Ge_2O_7$.

Keywords: ab initio, germanates, density functional theory, phonon spectrum

Much attention is paid to $R_2Ge_2O_7$ crystals (R is a rare earth ion) because of the variety of their properties [1–5]. They are crystallized into different structure types [1, 6]. The crystal structure of these compounds has been thoroughly studied [2, 7]; however, there are no experimental data on the phonon spectra and elastic constants for series rare-earth germanates. Rare-earth germanates are promising as scintillators [8]; yttrium germanate $Y_2Ge_2O_7$ is used as a matrix for doping by rare-earth ions [9, 10]. IR and Raman spectra of $Y_2Ge_2O_7$ were measured in [11]; however, the low-frequency spectral region (up to 200 cm^{-1}), which contains modes with the maximum degree of participation of yttrium ions, was not investigated. Thus, experimental data on the germanate modes with the maximum degree of participation of rare-earth ions is absent. Only 17 out of 48 IR-active modes and only 20 out of 81 Raman modes were determined in [11]. The measurements in [11] were performed using a polycrystalline sample, and the mode types were not experimentally determined. Thus, the known experimental data on IR and Raman spectra of yttrium germanate should be complemented and interpreted. Experimental data for other representatives of the series (R = Tb–Lu) are also absent. Specific features of the $Y_2Ge_2O_7$ structure were previously discussed in [12], where it was noted that yttrium germanate is crystallized into the sp. gr. $P4_32_12$ (it makes an enantiomorphic pair with the group $P4_12_12$, into which the entire series R = Tb–Lu is crystallized). Thus, the

crystal structure of yttrium germanate is similar to the specular reflection of the structure of rare-earth germanates $R_2Ge_2O_7$ (R = Tb–Lu).

It seems actual to ab initio investigate the phonon spectrum of rare-earth germanates $R_2Ge_2O_7$ (R = Tb–Lu, Y) with a tetragonal structure. The purpose of this study was to analyze within the unified ab initio approach the crystal structure, phonon spectrum, and elastic properties of a series of germanates $R_2Ge_2O_7$ (R = Tb–Lu, Y).

1. CALCULATION TECHNIQUES

Calculations were performed within the density functional theory and the approach of linear combination of atomic orbitals (MO LCAO). The hybrid functional PBE0 [13], which takes into account the contribution from nonlocal exchange (in the Hartree–Fock formalism), and non-dynamic correlations were used [14]. The calculations were carried out using the CRYSTAL17 program [15], which is designed for simulating periodic structures. Note that the phonon spectrum of germanates with a pyrochlore structure was calculated previously within the same approach [16].

Ge and O were described using the full-electron basis sets [17, 18]. The inner electron shells of rare-earth Tb–Lu and Y ions were described using the pseudopotentials from [19, 20]. Test calculations were performed by an example of $Gd_2Ge_2O_7$ with a

Table 1. Gd₂Ge₂O₇ lattice constant

Parameters	Calculation (ECP53)	Calculation (ECP28)	Experiment [22]
a , Å	10.053	9.991	9.999
Gd–O1, Å	2.505	2.482	2.535
Gd–O2, Å	2.177	2.163	2.165
ρ	0.869	0.871	0.854

pyrochlore structure using two pseudopotentials: ECP53MWB-1 [19], which replaces inner shells up to the $4f$ shell inclusively, and ECP28MWB_SEG [21], which replaces inner shells only up to the $3d$ shell and leaves the $4f$ shell in the valence balance (i.e., it enters the valence basis set in this case and is described directly). The results are compared in Table 1, which also contains the experimental data from [22]. Parameter $\rho = (\text{Gd–O2}/\text{Gd–O1})$ characterizes the degree of distortion of the octahedron with a rare-earth ion at the center and oxygen ions at the vertices. Reproduction of this parameter may serve as an estimate of adequacy of the used basis sets.

The use of the “short” pseudopotential (i.e., explicit description of the $4f$ shell using a basis set) somewhat improves reproduction of the lattice constant, but increases significantly the computing time, which is a critical factor for simulation of the low-symmetry structures under consideration.

In this study, inner shells of rare-earth ions were described using quasi-relativistic ECPnMWB pseudopotentials, where ECP is for “effective core potential”, WB is for “quasi-relativistic”, and n is the number of inner electrons replaced by the pseudopotential ($n = 54$ for Tb, 55 for Dy, etc.) [19, 23]. Thus, inner shells of a rare-earth ion (including $4f$) were replaced by the pseudopotential. The outer shells ($5s^25p^6$), involved in chemical bonds, were described using the ECPnMWB-I valence basis sets [23–25], which contain radial functions of the s , p , and d type. Pseudopotential ECP28MWB with a corresponding basis set was used for yttrium. The pseudopotentials and valence basis sets are available at the Stuttgart Group website [26]. Gaussian primitives with the exponential factors below 0.1 were removed from the valence basis sets, which is characteristic of periodic calculations.

The calculation algorithm was as follows. First, the crystal structure was optimized: the lattice constants and ionic coordinates in a cell were determined. The phonon spectrum (at the Γ point) or elastic constants were calculated for the obtained crystal structure corresponding to the energy minimum.

Integration over the Brillouin zone was performed using the Monkhorst–Pack scheme with a k -point grid $4 \times 4 \times 4$ in size. This grid was chosen based on

Table 2. Calculation of the crystal structure of tetragonal Er₂Ge₂O₇ using different grids

Grid	Lattice constant, Å		SCF energy, Hartree
$2 \times 2 \times 2$	a	6.84380243	–19027.960230
	c	12.43678912	
$4 \times 4 \times 4$	a	6.84377960	–19027.960928
	c	12.43704974	
$6 \times 6 \times 6$	a	6.84378081	–19027.960928
	c	12.43705748	
$8 \times 8 \times 8$	a	6.84378073	–19027.960928
	c	12.43707140	

the test calculations carried out for erbium germanate with a tetragonal structure (Er₂Ge₂O₇) (Table 2).

It should be noted that the energy of self-consistent field (SCF) was calculated with an accuracy of 10^{-6} Hartree. (Accuracy of calculating the two-electron integrals was no less than 10^{-7} Hartree.) As follows from the calculations, the $4 \times 4 \times 4$ grid is quite sufficient. At a finer grid, the SCF energies are retained accurate to the sixth decimal place. The lattice constants at a finer grid change at the fifth decimal place. This calculation accuracy can be assumed quite acceptable, because the difference in the calculated and experimental lattice constants is within 0.1 Å (a typical value for ab initio calculations).

2. CRYSTAL STRUCTURE

Rare-earth germanates R₂Ge₂O₇ (R = Tb–Lu) have a tetragonal crystal structure and belong to the sp. gr. $P4_12_12$ (92). A unit cell (Fig. 1) contains $Z = 4$ formula units and 44 atoms. R and Ge ions are surrounded by seven and four O atoms, respectively (Figs. 2, 3). The results of calculating the crystal structure are reported in Tables 3–6.

The ionic coordinates in a cell of Er₂Ge₂O₇ were determined by an X-ray diffraction (XRD) analysis. The calculation results and experimental data are compared in Table 4.

The results of calculating the crystal structure are in good agreement with the known experimental data. The lattice constants and bond lengths decrease along the Tb–Lu series, which corresponds to lanthanide compression. The R–O bond length shortens by 0.06 – 0.09 Å as moving from Tb to Lu. Note that the Ge–O bond length (O = O2, O3, and O4) shortens by 0.008 – 0.027 Å and the Ge–O1 bond length decreases by 0.08 Å. Thus, replacement of the rare-earth ion barely affects the Ge–O bonds (O = O2, O3, and O4), while the Ge–O1 bond changes similarly to the R–O

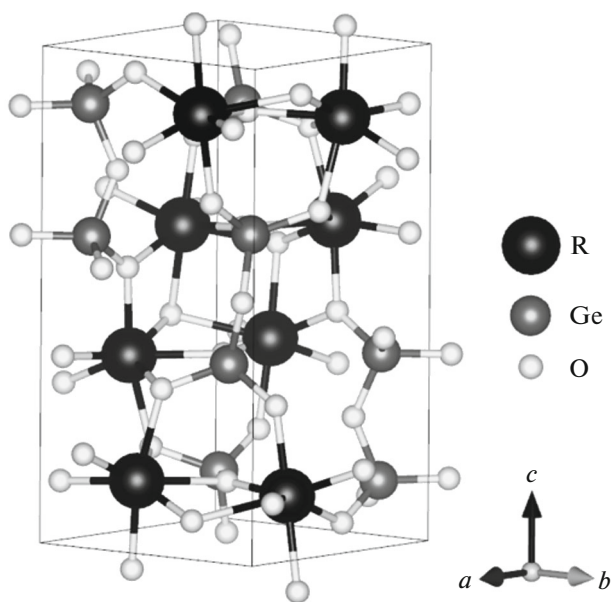


Fig. 1. $R_2Ge_2O_7$ unit cell: tetragonal structure, sp. gr. $P4_12_12$ (92).

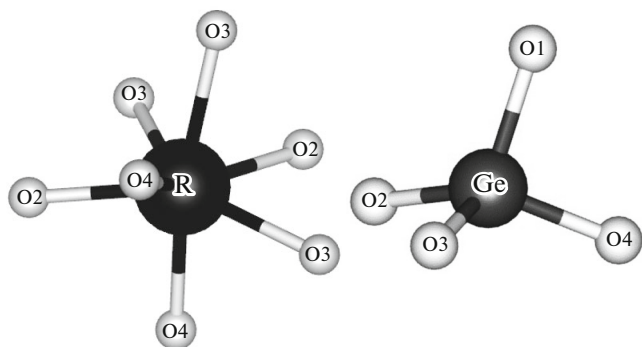


Fig. 2. R and Ge ions with their environments.

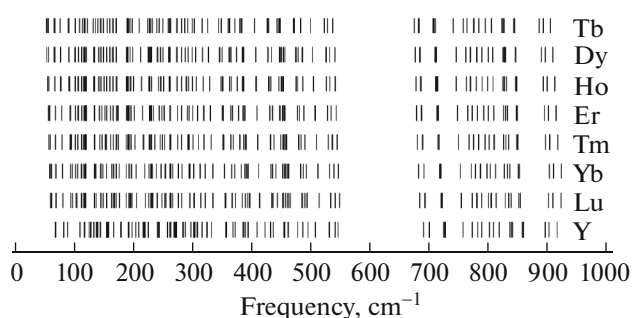


Fig. 3. Frequencies of the phonon modes of $R_2Ge_2O_7$ at the Γ point.

bond. Ion O1, in turn, bounds the centers of GeO_4 tetrahedra and is not the nearest neighbor of the rare earth ion.

3. VIBRATIONAL SPECTRUM

Germanates $R_2Ge_2O_7$ ($R = Tb-Lu, Y$) with a tetragonal structure are characterized by the following phonon modes at the Γ point:

$$\Gamma = 16A_1(R) + 17A_2(IR) + 17B_1(R) + 16B_2(R) + 33E(R, IR),$$

where R and IR are Raman and infra-red modes, respectively. Two modes are translational: one A_2 and one E (a doubly degenerate mode). The results of calculating the phonon modes at the Γ point, their types, and the IR and Raman intensities are listed in Tables 7 and 8. A change in the frequencies in the Tb-Lu series is shown in Fig. 3.

A comparison of the calculation results with the only known experimental data (for $Y_2Ge_2O_7$) demonstrates that they are in good agreement (Figs. 4, 5). The intensities of the Raman modes are calculated for the excitation wavelength of 488 nm and $T = 300$ K, which corresponds to the experimental conditions. The spectrum was simulated using Lorentzians with a half-width of 7 cm^{-1} . In [11], 20 Raman and 17 IR modes were experimentally found (the Raman mode at 790 cm^{-1} was determined by approximation). The mode types were not determined. The calculations supplement the experimental data [11], which do not include the low-frequency spectral range. An yttrium ion (a rare earth ion in the case of $R = Tb-Lu$) participates most actively in vibrations in specifically this range. The mode types indicated in Figs. 4 and 5 are obtained from the calculations.

The degrees of participation of ions in each mode were determined by analyzing the displacement vectors obtained from the ab initio calculation. The ionic displacements in each vibration for $Y_2Ge_2O_7$ and $Er_2Ge_2O_7$ are shown in Figs. 6 and 7, respectively.

According to the calculations, the strongest participations of Y and Ge ions are observed at frequencies 67 cm^{-1} (A_2 mode) and 88 cm^{-1} (E mode), respectively. The strongest participation of oxygen ions was predicted in the following modes: E mode with a frequency of 255 cm^{-1} (O1), E mode with a frequency of 216 cm^{-1} (O2 and O3), and A_2 mode with a frequency of 134 cm^{-1} (O4). Active participation of Y and Ge ions is observed in the modes with frequencies up to ~ 300 and $\sim 500\text{ cm}^{-1}$, respectively. An O ion participates actively in all modes.

The strongest IR mode (698 cm^{-1} , E mode) mainly involves ions O1 and O2. The strongest mode in the Raman spectrum is A_1 with a frequency of 857 cm^{-1} ,

Table 3. $R_2Ge_2O_7$ lattice constants (R = Tb–Lu, Y), Å

R		Calculation	Experiment	Δ
Tb	a	6.9167	6.8554 [7]	0.0613
	c	12.5787	12.4634	0.1153
Dy	a	6.8917	6.8269 [27]	0.0648
	c	12.5302	12.4289	0.1013
Ho	a	6.8675	6.8068 [27]	0.0589
	c	12.4836	12.3812	0.1024
Er	a	6.8438	6.7849 [28]	0.0589
	c	12.4371	12.3380	0.0991
Tm	a	6.8232	6.7645 [29]	0.0587
	c	12.3953	12.2930	0.1023
Yb	a	6.8011	6.7426 [7]	0.0585
	c	12.3496	12.2604	0.0892
Lu	a	6.7845	6.7278 [7]	0.0567
	c	12.3140	12.2246	0.0894
Y*	a	6.8196	6.8022 [12]	0.0174
	c	12.3955	12.3759	0.0196

* Calculation for yttrium germanate is performed in the enantiomorphic group $P4_32_12$, which corresponds to the experimental data.

Table 4. Coordinates of $Er_2Ge_2O_7$ ions, rel. units

Ion		Site	Calculation	Experiment [30]
Er	x	8a	0.8757	0.8756
	y		0.3521	0.3527
	z		0.1349	0.1355
Ge	x	8a	0.9015	0.9004
	y		0.1526	0.1521
	z		0.6193	0.6196
O1	x	4a	0.8061	0.055
	y		0.1939	0.1945
	z		0.7500	0.7500
O2	x	8a	0.0786	0.0764
	y		-0.0301	-0.0331
	z		0.6226	0.6236
O3	x	8a	0.0647	0.0638
	y		0.3377	0.3355
	z		0.5717	0.5751
O4	x	8a	0.6850	0.6833
	y		0.1452	0.1449
	z		0.5454	0.5427

in which ions O3 and O4 actively participate. In the second strongest Raman mode with a frequency of 455 cm^{-1} (also A_1), ion O4 participates most strongly. The high-frequency range ($\sim 700\text{--}900\text{ cm}^{-1}$) of both the IR and Raman spectra is due to the dominant participation of an oxygen ion. In the high-frequency

E mode (916 cm^{-1}), ion O4 participates most actively; however, this mode is weak.

In rare-earth germanates, active participation of rare-earth ions is observed in the low-frequency modes with frequencies up to $\sim 200\text{ cm}^{-1}$ ($\sim 400\text{ cm}^{-1}$

Table 5. Ion–ion distances, comparison with the experiment data (in Å)

Ion		Er		Tm		Y	
		calculation	experiment [30]	calculation	experiment [4]	calculation	experiment [12]
R–O	O2	2.2310	2.195	2.2224	2.197	2.2139	2.211
	O4	2.2613	2.216	2.2509	2.231	2.2499	2.245
	O4'	2.2878	2.266	2.2756	2.252	2.2762	2.279
	O3	2.3002	2.278	2.2901	2.273	2.2953	2.284
	O2'	2.3719	2.371	2.3613	2.345	2.3800	2.373
	O3'	2.4066	2.421	2.3924	2.362	2.3901	2.386
	O3''	2.5511	2.516	2.5418	2.540	2.5446	2.552
Ge–O	O2	1.7420	1.733	1.7420	1.740	1.7394	1.737
	O4	1.7442	1.751	1.7441	1.732	1.7407	1.733
	O1	1.7743	1.756	1.7729	1.751	1.7744	1.769
	O3	1.7894	1.754	1.7890	1.769	1.7850	1.780

Table 6. Calculated ion–ion distances in $R_2Ge_2O_7$ ($R = Tb-Lu, Y$), Å

Ion		Tb	Dy	Ho	Er	Tm	Yb	Lu	Y
R–O	O2	2.2619	2.2513	2.2412	2.2310	2.2224	2.2135	2.2068	2.2139
	O4	2.2977	2.2853	2.2729	2.2613	2.2509	2.2392	2.2307	2.2499
	O4'	2.3298	2.3151	2.3018	2.2878	2.2756	2.2628	2.2528	2.2762
	O3	2.3355	2.3231	2.3111	2.3002	2.2901	2.2788	2.2707	2.2953
	O2'	2.4079	2.3957	2.3836	2.3719	2.3613	2.3507	2.3417	2.3800
	O3'	2.4555	2.4385	2.4231	2.4066	2.3924	2.3779	2.3660	2.3901
	O3''	2.5856	2.5739	2.5621	2.5511	2.5418	2.5313	2.5243	2.5446
Ge–O	O2	1.7425	1.7423	1.7419	1.7420	1.7420	1.7417	1.7417	1.7394
	O4	1.7449	1.7447	1.7445	1.7442	1.7441	1.7437	1.7436	1.7407
	O1	1.7786	1.7771	1.7756	1.7743	1.7729	1.7716	1.7705	1.7744
	O3	1.7907	1.7902	1.7900	1.7894	1.7890	1.7884	1.7880	1.7850

for Ge). Oxygen participates in all modes. The frequencies of the strongest modes increase in the series from Tb to Lu within 11 cm^{-1} . The highest degree of participation of a rare earth ion in the Tb–Lu series is observed in the low-frequency modes and at a frequency of $103\text{--}107\text{ cm}^{-1}$ (E mode). The displacement value decreases with lanthanide compression. A germanium ion is characterized by the largest displacement at a frequency of $138\text{--}144\text{ cm}^{-1}$ (B_1 mode). Oxygen ions participate in all modes. The strongest participation of O ions in the series was predicted for the following modes: A_2 mode at frequencies in the range of $130\text{--}136\text{ cm}^{-1}$ (O1), A_2 mode at frequencies in the range of $190\text{--}195\text{ cm}^{-1}$ (O2), E mode at frequencies

in the range of $239\text{--}247\text{ cm}^{-1}$ in the Dy–Lu series, A_2 mode at a frequency of 344 cm^{-1} for Tb (O3), and E mode at frequencies in the range of $163\text{--}167\text{ cm}^{-1}$ (O4). Strong participation of oxygen ions is also observed in the high-frequency spectral range.

4. ELASTIC CONSTANTS

The results of calculating elastic constants, bulk modulus, shear modulus (according to Hill), and Vickers hardness are listed in Table 9. Hardness H_V was estimated from formula (1) from [31], where it was successfully used to describe a series of ~ 40 compounds with ionic and covalent bonds. As was noted in [31], this formula yields the best agreement with the experimental data at hardness more than 5 GPa. In

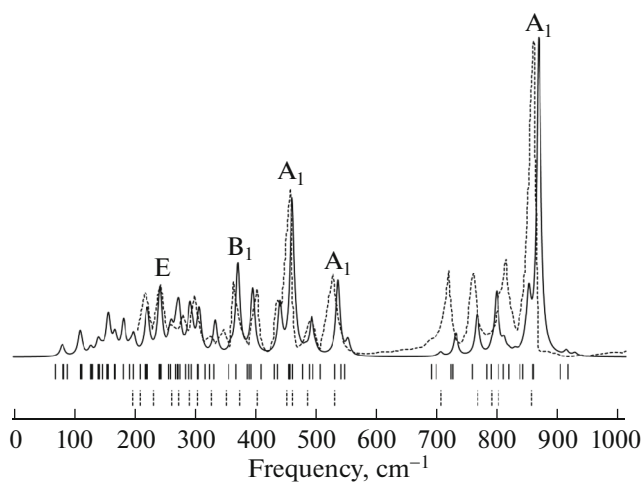


Fig. 4. Comparison of the (solid curve) calculated and (dashed curve) experimental [10] Raman spectra of $Y_2Ge_2O_7$.

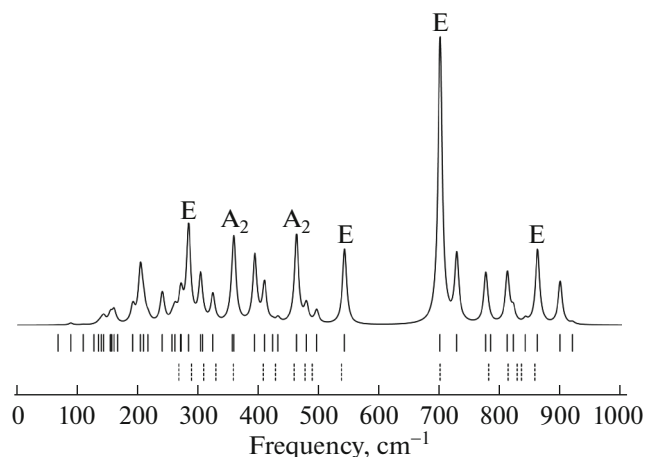


Fig. 5. Comparison of the (solid curve) calculated and (dashed curve) experimental [10] IR spectra of $Y_2Ge_2O_7$.

Table 7. Phonon modes of $Y_2Ge_2O_7$

Frequency, cm^{-1}	Type	IR intensity, km/mol	Raman intensity, rel. units	Frequency, cm^{-1}	Type	IR intensity, km/mol	Raman intensity, rel. units
67	A ₂	5	—	314	B ₂	—	0.02
68	B ₁	—	0	323	E	627	0.85
79	A ₁	—	22	330	A ₁	—	104
81	B ₂	—	17	355	E	413	19
88	E	43	0.02	357	A ₂	1697	—
109	E	10	73	366	B ₂	—	0.34
111	B ₁	—	9	367	B ₁	—	287
126	B ₂	—	6	384	A ₁	—	3
127	E	3	16	388	B ₂	—	21
129	A ₁	—	1.07	391	E	3	192
134	A ₂	35	—	392	A ₂	1527	—
138	E	68	37	408	E	891	0.92
140	B ₁	—	9	421	A ₂	33	—
142	A ₂	160	—	430	E	108	0.16
145	B ₁	—	14	435	A ₁	—	154
153	E	201	14	453	B ₁	—	54
155.5	E	16	0.06	454	B ₂	—	13
155.7	A ₁	—	113	455	A ₁	—	422
160	A ₂	282	—	460	E	536	32
165.5	E	8	21	461	A ₂	1496	—
166.3	A ₁	—	38	477	E	407	11
180	B ₂	—	104	487	B ₁	—	111
190.2	A ₂	17	—	494	E	288	11
190.4	E	365	0.93	506	B ₂	—	0.46
190.8	B ₁	—	15	530	A ₁	—	236
197	B ₂	—	58	540	E	1701	0.79
203	A ₂	1224	—	546	B ₂	—	44
208	E	339	1.28	690	A ₁	—	2
215.6	E	126	0.18	697.5	E	6544	11
216	B ₁	—	17	697.7	B ₁	—	2
217.6	B ₂	—	58	722	B ₂	—	71
218	B ₁	—	13	724.9	E	16	0.82
220	A ₁	—	67	725	A ₂	1497	—
239	E	682	176	757	B ₁	—	130
240	A ₁	—	33	773	A ₂	1148	—
242	B ₁	—	0.06	781	E	0.36	17
255	E	102	29	789	A ₁	—	195
258	B ₂	—	58	801	B ₂	—	38
260	A ₂	276	—	809	E	1145	9
266	A ₁	—	61	818	E	295	10
269	E	349	42	836	B ₂	—	19
270	E	318	87	838	A ₂	91	—
273	B ₁	—	3	841	B ₁	—	167
282	E	2190	12.36	857	A ₁	—	1000
288	B ₂	—	124	858	E	1695	6
292	A ₁	—	46	896	A ₂	966	—
302	E	1048	35	903	B ₁	—	15
304	B ₁	—	104	916	E	45	10
306	A ₂	27	—				

Table 8. Phonon modes of Er₂Ge₂O₇

Frequency, cm ⁻¹	Type	IR intensity, km/mol	Raman intensity, rel. units	Frequency, cm ⁻¹	Type	IR intensity, km/mol	Raman intensity, rel. units
56	A ₂	5	—	308	B ₂	—	0.18
58	B ₁	—	0.78	318	E	864	1
67.1	B ₂	—	20	330	A ₁	—	76
67.2	A ₁	—	4	349	A ₂	1683	—
78	E	26	3	352	E	359	16
92	B ₁	—	2	363	B ₂	—	0.03
93	E	0.96	71	367	B ₁	—	303
101	A ₁	—	8	378	A ₁	—	0.26
106	E	0.26	88	385	A ₂	1536	—
112	E	9	13	387.8	B ₂	—	31
116	B ₂	—	37	387.9	E	11	184
117	B ₁	—	40	409	E	953	1
119	A ₂	165	—	430	A ₂	131	—
120	A ₁	—	72	430.4	E	53	0.03
133	A ₂	105	—	435	A ₁	—	198
134	E	5	18	447	B ₂	—	12
141.7	E	212	2	451	A ₁	—	416
142.8	B ₁	—	0.2	453	B ₁	—	80
146	E	92	9	455	E	327	37
151	A ₂	142	—	456	A ₂	1039	—
155	B ₂	—	19	477	E	760	7
161	A ₁	—	47	481	B ₁	—	118
165	E	279	6	488	E	496	16
166	B ₁	—	0.05	507	B ₂	—	3
171	A ₂	52	—	528	A ₁	—	236
173	B ₂	—	68	534	E	1509	1
188	E	740	0	543	B ₂	—	42
190	B ₂	—	50	679	A ₁	—	2
191	A ₂	1274	—	687	B ₁	—	3
192	B ₁	—	31	688	E	6284	11
195	A ₁	—	74	713	B ₂	—	77
201	E	28	0.12	715	E	24	1
215	B ₁	—	8	716	A ₂	1382	—
226	B ₁	—	0.12	748	B ₁	—	136
227	E	717	58	765	A ₂	1148	—
229	B ₂	—	9	773	E	0.02	15
230	A ₂	19	—	782	A ₁	—	200
233	A ₁	—	42	793	B ₂	—	37
243	E	190	67	800	E	1161	8
247	E	233	148	809	E	379	8
252	A ₁	—	59	826	B ₂	—	20
261.37	E	71	43	829	A ₂	98	—
261.38	B ₁	—	21	833	B ₁	—	165
262	B ₂	—	249	848	A ₁	—	1000
274	E	28	42	849	E	1551	6
281	E	1905	15	895	A ₂	1087	—
290	A ₂	37	—	902	B ₁	—	16
293	A ₁	—	71	915	E	50	12
300	B ₁	—	69				

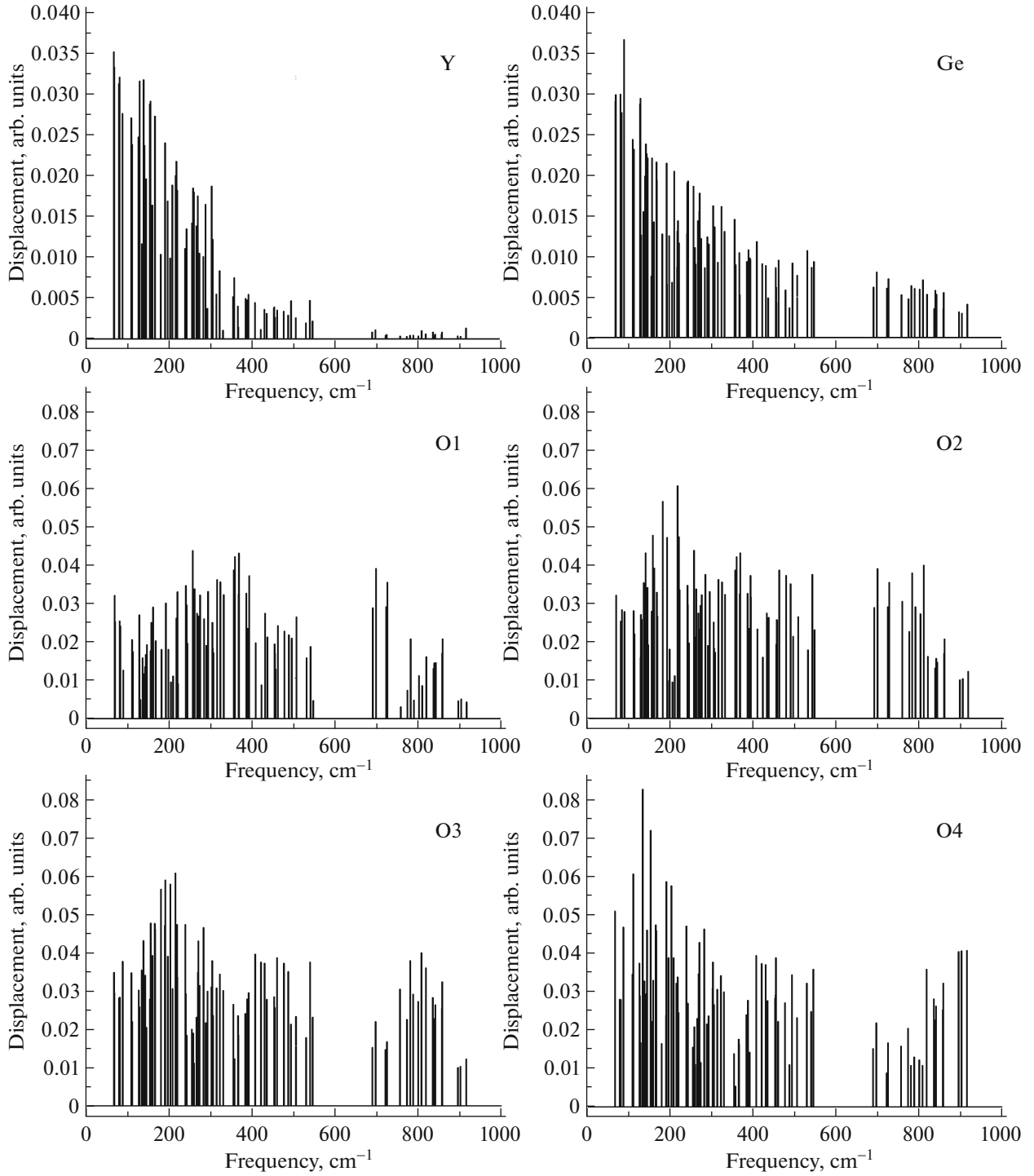


Fig. 6. Ionic displacements in the phonon modes for $Y_2Ge_2O_7$.

formula (1), B is the bulk modulus and G is the shear modulus.

$$H_V = 0.92 \left(\frac{G}{B} \right)^{1.137} G^{0.708}. \quad (1)$$

According to the calculations, all elastic constants in the Tb–Lu series increase with lanthanide compression (except for C_{12} , which decreases). The H_V value calculated from formula (1) increases.

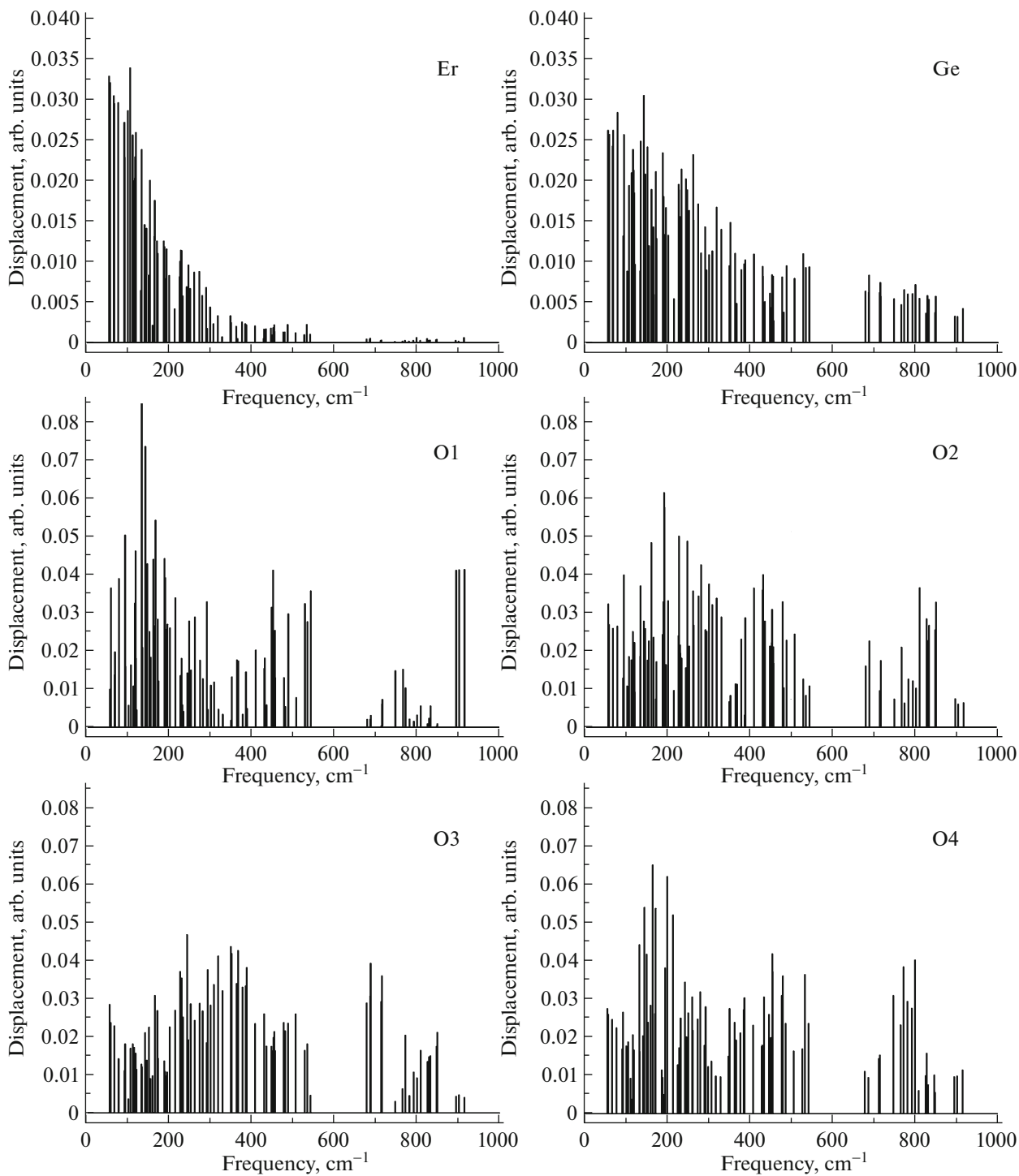


Fig. 7. Ionic displacements in the phonon modes for $\text{Er}_2\text{Ge}_2\text{O}_7$.

5. CONCLUSIONS

The crystal structures, phonon spectra at the Γ point, and elastic properties of a series of tetragonal germanates $\text{R}_2\text{Ge}_2\text{O}_7$ ($\text{R} = \text{Tb} - \text{Lu}, \text{Y}$) were calculated within the density functional theory and the MO LCAO approach. The frequencies and types of funda-

mental vibrations and the intensities of the IR and Raman modes were determined. The degrees of participation of ions in each mode were determined by analyzing the displacement vectors obtained as a result of ab initio calculations. The results of measuring the IR and Raman spectra of yttrium germanate $\text{Y}_2\text{Ge}_2\text{O}_7$

Table 9. Elastic constants, bulk modulus, shear modulus, and hardness of $R_2Ge_2O_7$ ($R = Tb-Lu, Y$), GPa

R	Tb	Dy	Ho	Er	Tm	Yb	Lu	Y
C_{11}	251	257	261	266	270	275	278	258
C_{12}	93	92	91	91	90	90	90	79
C_{13}	79	80	81	83	84	85	86	76
C_{33}	268	271	274	277	279	281	284	271
C_{44}	37	39	41	43	44	46	48	44
C_{66}	52	54	56	57	58	60	61	59
B	141	143	145	147	148	150	152	139
G	56	58	60	62	63	65	67	63
H_V	5.50	5.80	6.08	6.35	6.60	6.86	7.05	7.02

were supplemented, and the types of modes were determined; the results obtained can be used to interpret the spectra of isostructural germanates.

FUNDING

This study was supported by the Ministry of Science and Higher Education of the Russian Federation (project no. FEUZ-2020-0054).

CONFLICT OF INTEREST

The authors declare that they have no conflicts of interest.

REFERENCES

- G. Bocquillon, C. Chateau, and J. Lories, in *The Rare Earths in Modern Science and Technology, Proceedings of the Conference, June 25–28, 1979, Fargo, ND* (Springer, New York, 1980), p. 209.
- E. Morosan, J. A. Fleitman, Q. Huang, J. W. Lynn, Y. Chen, X. Ke, M. L. Dahlberg, P. Schiffer, C. R. Crayley, and R. J. Cava, *Phys. Rev. B* **77**, 224423 (2008).
- Q. Li, S. Zhang, W. Lin, W. Li, Y. Li, Z. Mu, and F. Wu, *Spectrochim. Acta, Part A* **228**, 117755 (2020).
- K. Stadnicka, A. M. Glazer, M. Koralewski, and B. M. Wanklyn, *J. Phys.: Condens. Matter* **2**, 4795 (1990).
- I. Yaeger, R. Shuker, and B. M. Wanklyn, *Phys. Status Solidi B* **104**, 621 (1981).
- L. N. Dem'yanets, *Hermanates of Rare Earth Elements* (Nauka, Moscow, 1980) [in Russian].
- L. T. Denisova, Y. F. Kargin, N. V. Belousova, L. A. Irtyugo, V. M. Denisov, and V. V. Beletskii, *Inorg. Mater.* **55**, 952 (2019).
- S. Kurosawa, T. Shishido, T. Sugawara, K. Yubuta, P. Jan, A. Suzuki, Y. Yokota, Y. Shoji, K. Kamada, and A. Yoshikawa, *J. Cryst. Growth* **393**, 142 (2014).
- K. Das, D. Ghosh, and B. M. Wanklyn, *J. Phys.: Condens. Matter* **11**, 1745 (1999).
- F. Zhao, P. Guo, G. Li, F. Liao, S. Tian, and X. Jing, *Mater. Res. Bull.* **38**, 931 (2003).
- R. Saez-Puche, M. Bijkerk, F. Fernández, E. J. Baran, and I. L. Botto, *J. Alloys Compd.* **184**, 25 (1992).
- G. J. Redhammer, G. Roth, and G. Amthauer, *Acta Crystallogr., C* **63** (10), i93 (2007).
- C. Adamo and V. Toward, *J. Chem. Phys.* **110**, 6158 (1999).
- A. V. Arbuznikov, *J. Struct. Chem.* **48**, S1 (2007).
- R. Dovesi, A. Erba, R. Orlando, C. M. Zicovich, Wilson, B. Civalleri, L. Maschio, M. Rérat, S. Casassa, J. Baima, S. Salustro, and B. Kirtman, *Wiley Interdiscipl. Rev.: Comput. Mol. Sci.* **8** (4), e1360 (2018).
- V. A. Chernyshev and N. M. Avram, *AIP Conf. Proc.* **2218**, 040004 (2020).
- G. Sophia, P. Baranek, C. Sarrazin, M. Rerat, and R. Dovesi, https://www.crystal.unito.it/Basis_Sets/germanium.html. Accessed 2014.
- F. Corá, *Mol. Phys.* **103**, 2483 (2005).
- M. Dolg, H. Stoll, A. Savin, and H. Preuss, *Theor. Chim. Acta* **75**, 173 (1989).
- D. Andrae, U. Haeussermann, M. Dolg, H. Stoll, and H. Preuss, *Theor. Chim. Acta* **77**, 123 (1990).
- X. Cao and M. Dolg, *J. Mol. Struct.: THEOCHEM* **581**, 139 (2002).
- X. Li, Y. Q. Cai, Q. Cui, C. J. Lin, Z. L. Dun, K. Matsubayashi, Y. Uwatoko, Y. Sato, T. Kawae, S. J. Lv, C. Q. Jin, J.-S. Zhou, J. B. Goodenough, H. D. Zhou, and J.-G. Cheng, *Phys. Rev. B* **94**, 214429 (2016).
- M. Dolg, H. Stoll, and H. Preuss, *Theor. Chim. Acta* **85**, 441 (1993).
- J. Yang and M. Dolg, *Theor. Chem. Acc.* **113**, 212 (2005).
- A. Weigand, X. Cao, J. Yang, and M. Dolg, *Theor. Chem. Acc.* **126**, 117 (2010).
- <http://www.tc.uni-koeln.de/PP/clickpse.en.html>.
- L. T. Denisova, L. A. Irtyugo, Y. F. Kargin, N. V. Belousova, V. V. Beletskii, and V. M. Denisov, *Inorg. Mater.* **54**, 361 (2018).
- L. T. Denisova, L. A. Irtyugo, V. V. Beletskii, N. V. Belousova, and V. M. Denisov, *Phys. Solid State* **61**, 537 (2019).
- L. T. Denisova, L. A. Irtyugo, N. V. Belousova, V. V. Beletskii, and V. M. Denisov, *Russ. J. Phys. Chem. A* **93**, 598 (2019).
- Y. I. Smolin, *Sov. Phys. Crystallogr.* **15**, 36 (1970).
- Y. Tian, B. Xu, and Z. Zhao, *Int. J. Refract. Met. Hard Mater.* **33**, 93 (2012).